

The crystal structure gives direct evidence for the existence of the Cu^{I} species in the substituted pyridine/ CuBr_2/HBr system. Unfortunately, the isolated mixed-valence species did not contain a brominated pyridine-ring system. Hence, it is not possible to tie the existence of the Cu^{I} ion to the bromination process. Indeed, the Cu^{I} ion may be simply generated by an inorganic reaction involving the decomposition of CuBr_2 to CuBr and Br_2 . Nevertheless, the crystallization of organoammonium halocuprate(II) salts under anaerobic conditions appears to be a general method leading to the formation of mixed-valence copper halide systems.

The authors acknowledge the support of NSF grant DMR-8219430. In addition, the X-ray diffraction facility was established through funds supplied by NSF grant CHE-8408407 and by The Boeing Company.

Acta Cryst. (1988). C44, 2071–2076

Structures of Ethylenediammonium Tetrabromocuprate(II) and Propylenediammonium Tetrabromocuprate(II)

BY KRIS HALVORSON AND ROGER D. WILLETT

Department of Chemistry, Washington State University, Pullman, Washington 99164, USA

(Received 29 January 1988; accepted 18 July 1988)

Abstract. $[\text{C}_2\text{H}_{10}\text{N}_2][\text{CuBr}_4]$, $M_r = 445.3$, monoclinic, $P2_1/a$, $a = 7.511$ (1), $b = 7.803$ (1), $c = 8.334$ (2) Å, $\beta = 92.12$ (2)°, $V = 488.1$ (1) Å³, $Z = 2$, $D_x = 3.02$ g cm⁻³, $F(000) = 410$, $\mu = 184.0$ cm⁻¹, numerical absorption correction, $T = 293$ K, 1417 unique reflections with $I > 3\sigma(I)$ refined to $R = 0.0504$ ($wR = 0.0392$). $[\text{C}_3\text{H}_{12}\text{N}_2][\text{CuBr}_4]$, $M_r = 459.3$, monoclinic, $P2_1/n$, $a = 8.086$ (2), $b = 7.566$ (2), $c = 17.622$ (5) Å, $\beta = 96.75$ (2)°, $V = 1071$ (1) Å³, $Z = 4$, $D_x = 2.85$ g cm⁻³, $F(000) = 852$, $\mu = 167.6$ cm⁻¹, empirical absorption correction assuming laminar crystal shape, $T = 293$ K, 864 unique reflections with $I > 3\sigma(I)$ refined to $R = 0.0359$ ($wR = 0.0473$). Both structures consist of antiferrodistortive perovskite layers with corner-shared Jahn–Teller elongated CuBr_6 octahedra with adjacent layers linked by the diammonium cations. The short Cu–Br distances average 2.440 Å while the longer semi-coordinate distances are 3.034 and 3.148 Å respectively for the two salts. The ethylenediammonium cation is in an all-*trans* conformation while the propylene analog has one *trans* and one *gauche* segment for a *tg* conformation. The layers are in a partially eclipsed conformation, leading to short interlayer Br...Br contacts of

References

- BLANCHETTE, J. & WILLETT, R. D. (1988). *Inorg. Chem.* **27**, 843–849.
 CAMPANA, C. F., SHEPHERD, D. F. & LITCHMAN, W. N. (1981). *Inorg. Chem.* **20**, 4039–4044.
 GEISER, U., GAURA, R., WILLETT, R. D. & WEST, D. X. (1987). *Inorg. Chem.* **26**, 4203–4212.
 PLACE, H. (1986). MS Thesis, Washington State Univ., USA.
 PLACE, H. & WILLETT, R. D. (1987). *Acta Cryst.* C43, 1497–1500.
 PLACE, H. & WILLETT, R. D. (1988). *Acta Cryst.* C44, 34–38.
 ROBIN, M. B. & DAY, P. (1967). *Adv. Inorg. Chem. Radiochem.* **10**, 247–422.
 SHELDRIK, G. M. (1986). *SHELXTL*, version 5.1. Nicolet Analytical Instruments, Madison, WI, USA.
 WILLETT, R. D. (1987). *Inorg. Chem.* **26**, 3423–3424.
 WILLETT, R. D., GEISER, U. & RAMAKRISHNA, B. L. (1988). *J. Magn. Res.* Submitted.
 WILLETT, R. D., GRIGERIT, T., HALVORSON, K. & SCOTT, B. (1987). *Proc. Indian Acad. Sci. (Chem. Sci.)* **98**, 147–160.
 WILLETT, R. D. & WEST, D. X. (1987). *Acta Cryst.* C43, 2300–2303.

3.602 and 4.065 Å respectively. Correlations between the structural parameters and magnetic behavior are discussed.

Introduction. Compounds of the type $A_2\text{CuX}_4$, where A^+ = alkali metal ion or a monosubstituted ammonium ion and $X = \text{Cl}^-$ or Br^- , typically form antiferrodistortive versions of the two-dimensional layer perovskite family (Steadman & Willett, 1970; Barendregt & Schenk, 1970; Larsen, 1974; Willett, 1964). In these compounds, adjacent layers are staggered with respect to each other, e.g. Cu ions in one layer are aligned above (or below) the A^+ cations on adjacent layers. In this manner, essentially no superexchange coupling can occur between layers, and dipolar interactions essentially cancel, leading to the formation of nearly ideal two-dimensional magnetic systems (de Jongh & Miedema, 1974). With the replacement of two A^+ cations by a diammonium cation, $^+\text{H}_3\text{NC}_n\text{H}_{2n}\text{NH}_3^+$, adjacent layers are now eclipsed in the sense that the copper ions in adjacent layers lie nearly directly above each other (Phelps, Losee, Hatfield & Hodgson, 1976; Ferguson & Zaslow, 1971; Tichy, Benes, Hälgl & Arend, 1978). This allows for magnetic interactions to

Table 1. X-ray data collection parameters

	Ethylenediammonium tetrabromocuprate(II) Nicolet R3m/E	Propylenediammonium tetrabromocuprate(II) Upgraded Syntex P2 ₁
Diffractometer system	Nicolet R3m/E	Upgraded Syntex P2 ₁
Systematic absences	<i>h</i> odd for <i>h</i> 0l <i>k</i> odd for 0k0	<i>h</i> + 1 odd for <i>h</i> 0l <i>k</i> odd for 0k0
Lattice constants	Based on 25 reflections in the range 26 < 2θ < 37°	Based on 25 reflections in the range 20 < 2θ < 32.5°
Crystal size (mm)	0.48 × 0.25 × 0.042	0.12 × 0.6 × 0.2
Type of absorption correction	Numerical	Laminar
Transmission range	0.110–0.442	0.346–0.913
Check reflections	220, 221	040, 220
Total reflections	1653	1010
(sinθ/λ)(max) (Å ⁻¹)	0.703	0.538
Unique reflections	1417 with 1094 with <i>F</i> > 3σ	864 with 654 with <i>F</i> > 3σ
<i>R</i> for equivalent reflections	0.0218	0.0157
Structure solution package	Nicolet SHELXTL (Sheldrick, 1985)	Nicolet SHELXTL (Sheldrick, 1985)
Structure solution technique	Direct methods	Direct methods
<i>R</i>	0.0504	0.0359
<i>wR</i>	0.0392	0.0473
<i>w</i> = 1/[σ ² (<i>F</i>) + <i>g</i> (<i>F</i>) ²]	<i>g</i> = 0.00011	<i>g</i> = 0.00246
Δ σ _(mean)	0.001	0.013
Δ σ _(max)	0.004	0.045
Total parameters refined	44	69
Thermal parameters	Anisotropic on all non-hydrogen atoms	Anisotropic on Cu and Br atoms
H atoms	Constrained to C–H and N–H = 0.96 Å, thermal parameters fixed at 1.2 <i>U</i> _{eq} for the heavier atom	Constrained to C–H and N–H = 0.96 Å, thermal parameters fixed at 1.2 <i>U</i> _{eq} for the heavier atom
Largest peak on final difference map (e Å ⁻³)	1.21 near Br(1)	0.64 near 0,0,0 special position
Extinction corrections	Yes	None
Goodness of fit	1.302	0.885

occur *via* Cu–X···X–Cu pathways which, for small *n*, may become quite significant. The effect is substantially larger for X = Br⁻ than for X = Cl⁻ since the interlayer distance is effectively fixed by the length of the C_{*n*}H_{2*n*} segment. However, the substantial increase in ionic radius leads to a larger overlap of electron density and thus to a stronger magnetic coupling (Snively, Seifert, Emerson & Drumheller, 1979; Snively, Tuthill & Drumheller, 1981; Block & Jansen, 1982; Rubenacker, Waplak, Hutton, Haines & Drumheller, 1985; Garland, Emerson & Pressprich, 1989). Since the structures of the first two members of the bromide series, (NH₃-C₂H₄NH₃)CuBr₄ and (NH₃C₃H₆NH₃)CuBr₄, have not been determined, crystal structure analyses have been undertaken to determine the structural parameters associated with the Cu–Br···Br–Cu pathways, as well as details of the intralayer structure.

Experimental. Polycrystalline samples of (C₂H₄N₂-H₆)CuBr₄ and (C₃H₆N₂H₆)CuBr₄ were prepared by partial evaporation of a 1:1 mixture of the appropriate diamine and CuBr₂ in dilute HBr solution. Single crystals for X-ray analysis were grown by a modified thermal gradient technique (Arend, Huber, Miskovsky & Van Leeuwen, 1978). The crystals, in general, tend to be badly twinned and exhibit large mosaic spreads. This is typical of the diammonium salts (Tichy *et al.*, 1978). After considerable searching however, satisfactory single crystals were obtained for the X-ray data collection.

Table 2. Final positional parameters (× 10⁴) and isotropic or equivalent isotropic thermal parameters (× 10³)

	<i>x</i>	<i>y</i>	<i>z</i>	<i>U</i> / <i>U</i> _{eq} (Å ²)
(C ₂ H ₄ N ₂ H ₆)CuBr ₄				
Cu	0	0	0	22 (1)†
Br(1)	2664 (1)	-2905 (1)	403 (1)	30 (1)†
Br(2)	284 (1)	435 (1)	2903 (1)	31 (1)†
N	5022 (8)	-246 (7)	7258 (7)	32 (2)†
C	4545 (11)	483 (10)	5639 (8)	36 (3)†
(C ₃ H ₆ N ₂ H ₆)CuBr ₄				
Cu(1)	0	0	0	36 (3)†
Br(1)	-2068 (3)	2241 (4)	215 (2)	39 (2)†
Br(2)	835 (3)	-186 (4)	1374 (2)	42 (2)†
Cu(2)	-5000	5000	0	35 (3)†
Br(3)	-7155 (3)	2749 (4)	-191 (2)	37 (2)†
Br(4)	-4863 (4)	5147 (4)	-1380 (2)	43 (2)†
N(1)*	-7 (2)	507 (3)	378 (1)	34 (7)
C(2)*	-117 (3)	467 (4)	309 (2)	49 (10)
C(3)*	-71 (5)	550 (6)	235 (2)	127 (16)
C(4)*	54 (6)	477 (6)	202 (3)	155 (20)
N(5)*	60 (3)	504 (3)	121 (2)	54 (8)

* Parameters listed are multiplied by 10³.

† Equivalent thermal *U* defined as one-third of the trace of the orthogonalized *U*_{*ij*} tensor.

Data collection (Campana, Shepherd & Litchman, 1981) with either a Nicolet R3m/E diffractometer or a Syntex P2₁ diffractometer upgraded to Nicolet P3F specifications. Mo *K*α radiation. λ = 0.71069 Å. Graphite monochromator. Data collection details given in Table 1. Structure solution *via* direct methods (Sheldrick, 1985) with C, N and H atoms located on difference synthesis maps. For the propylenediammonium salt, it was apparent from the thermal parameters that two of the carbon atoms [C(3) and C(4)] were disordered. However, attempts to locate and refine individual sites for the disordered atoms were unsuccessful. For this reason, all C and N atoms were refined with isotropic thermal parameters. Refinement *via* blocked-diagonal cascading least-squares procedure. Scattering factors with dispersion corrections from *International Tables for X-ray Crystallography* (1974). H atoms constrained to idealized positions with isotropic thermal parameters fixed at approximately 20% larger than the corresponding heavier atom. Details summarized in Table 1. Final positional parameters and equivalent isotropic thermal parameters are listed in Table 2, pertinent bond distances and angles in Table 3, with interlayer and hydrogen-bonding contacts listed in Table 4.*

Discussion. Both structures consist of layers of square-planar CuBr₄²⁻ ions linked together by semi-coordinate

* Lists of structure factors, anisotropic thermal parameters and H-atom parameters have been deposited with the British Library Document Supply Centre as Supplementary Publication No. SUP 51256 (16 pp.). Copies may be obtained through The Executive Secretary, International Union of Crystallography, 5 Abbey Square, Chester CH1 2HU, England.

Table 3. Bond distances (Å) and angles (°)

$(C_2H_4N_2H_6)CuBr_4$			
Cu—Br(1)	2.431 (1)	N—C	1.496 (9)
Cu—Br(2)	2.444 (1)	C—C ⁱⁱ	1.492 (15)
Cu—Br(1)	3.034 (1)		
Br(1)—Cu—Br(2)	90.4 (1)	N—C—C ⁱⁱ	110.5 (8)
Cu—Br(1)—Cu ⁱ	164.5 (1)		
$(C_3H_6N_2H_6)CuBr_4$			
Cu(1)—Br(1)	2.442 (3)	Cu(2)—Br(1)	3.148 (3)
Cu(1)—Br(2)	2.440 (3)	N(1)—C(2)	1.44 (4)
Cu(1)—Br(3 ⁱⁱⁱ)	3.148 (3)	C(2)—C(3)	1.55 (5)
Cu(2)—Br(3)	2.432 (3)	C(3)—C(4)	1.34 (7)
Cu(2)—Br(4)	2.450 (3)	C(4)—N(5)	1.46 (6)
Br(1)—Cu(1)—Br(2)	90.0 (1)	N(1)—C(2)—C(3)	116 (3)
Br(3)—Cu(2)—Br(4)	90.5 (1)	C(2)—C(3)—C(4)	116 (4)
Cu(1)—Br(3 ⁱⁱⁱ)—Cu(2 ⁱⁱⁱ)	165.6 (1)	C(3)—C(4)—N(5)	119 (4)
Cu(2)—Br(1)—Cu(1 ⁱⁱⁱ)	164.0 (1)		

Symmetry codes: (i) $0.5-x, -y, -z$; (ii) $1-x, -y, 1-z$; (iii) $1+x, y, z$.

Table 4. Interlayer and primary hydrogen-bonding contacts (Å, °)

$(C_2H_4N_2H_6)CuBr_4$			
Br(2)—Br(2 ⁱ)	3.602 (1)	H(1C)—Br(2 ⁱⁱⁱ)	2.458
N(1)—Br(1 ⁱⁱ)	3.391 (2)	N(1)—Br(2 ^{iv})	3.536 (2)
H(1A)—Br(1 ⁱⁱ)	2.452	H(1B)—Br(2 ^{iv})	2.611
Cu—Br(2)—Br(2 ⁱ)	155.7 (1)	N(1)—H(1 ⁱⁱⁱ)—Br(2 ⁱⁱⁱ)	161.2
C(1)—N(1)—Br(1 ⁱⁱ)	100.7 (4)	C(1)—N(1)—Br(1 ⁱⁱ)	100.7 (4)
N(1)—H(1A)—Br(1 ⁱⁱ)	165.7	N(1)—H(1B)—Br(2 ^{iv})	162.0
C(1)—N(1)—Br(2 ⁱⁱⁱ)	109.3 (4)		
$(C_3H_6N_2H_6)CuBr_4$			
Br(2 ^v)—Br(4)	4.063 (3)	N(1)—Br(2 ^{viii})	3.473 (5)
N(5)—Br(2 ^{vi})	3.624 (5)	H(1C)—Br(2 ^{viii})	2.550
H(5B)—Br(2 ^{vi})	2.704	N(1)—Br(3 ^{ix})	3.377 (4)
N(5)—Br(1)	3.365 (5)	H(1A)—Br(3 ^{ix})	2.508
H(5C)—Br(1)	2.503	N(1)—Br(4 ^x)	3.666 (5)
N(5)—Br(3 ^{vii})	3.547 (5)	H(1B)—Br(4 ^x)	2.709
H(5A)—Br(3 ^{vii})	2.828		
Cu(1)—Br(2)—Br(4)	155.8 (2)	N(5)—H(5A)—Br(3 ^{vii})	147.0
Cu(2)—Br(4)—Br(2)	174.2 (2)	C(2)—N(1)—Br(2 ^{viii})	116.2 (6)
C(4)—N(5)—Br(2 ^{vi})	94.0 (8)	N(1)—H(1C)—Br(2 ^{viii})	161.2
N(5)—H(5B)—Br(2 ^{vi})	160.8	C(2)—N(1)—Br(3 ^{ix})	90.8 (8)
C(4)—N(5)—Br(1)	109.4 (7)	N(1)—H(1A)—Br(3 ^{ix})	150.5
N(5)—H(5C)—Br(1)	149.5	C(2)—N(1)—Br(4 ^x)	100.3 (6)
C(4)—N(5)—Br(3 ^{vii})	116.8 (7)	N(1)—H(1B)—Br(4 ^x)	161.7

Symmetry codes: (i) $x, y, -1+z$; (ii) $0.5-x, 0.5+y, 1-z$; (iii) $0.5-x, -0.5+y, 1-z$; (iv) $1-x, -y, 1-z$; (v) $-0.5+x, 0.5-y, -0.5+z$; (vi) $x, 1+y, z$; (vii) $-x, 1-y, -z$; (viii) $0.5-x, 0.5+y, 0.5-z$; (ix) $0.5+x, 0.5-y, 0.5+z$; (x) $0.5+x, 1.5-y, 0.5+z$.

Cu...Br bonds with the latter completing the Jahn-Teller elongated octahedral coordination geometry for the Cu^{II} ions. Adjacent layers are bridged by the diammonium cations, providing three-dimensional stability to the lattice. Distances within the anions average 2.440 Å with semi-coordinate bond lengths averaging 3.034 and 3.148 Å for the C₂ and C₃ compounds respectively. The bridging Cu—Br...Cu angles range from 164.0 (1) to 165.6 (1)°. This non-linearity of the bridging linkages (shown in Fig. 1 for the C₃ compound) leads to the typical puckering or

'washboard' effect in the layer structure. This is due to the hydrogen bonding between the diammonium ions and the layers.

The ethylenediammonium structure is isomorphous with the corresponding chloride salt (Tichy *et al.*, 1978) with the slight increase in unit-cell size (0.2–0.4 Å per edge) consistent with the larger radius for the Br ion. Many details appear relatively unchanged. The CuBr₄²⁻ anions lie on centers of inversion, and so are rigorously planar. Both coordinate and semi-coordinate Cu—X bonds are approximately 0.15 Å longer in the Br salt, the increase being equal to the difference in ionic radii of the two halide ions. The ethylenediammonium ions lie on centers of inversion, causing adjacent layers to shift slightly (0.28 Å) so that the non-bridging bromide ions on adjacent layers are not totally eclipsed. As can be seen from Fig. 2, the —NH₃ groups interact with the layer such that two N—H...Br hydrogen bonds are formed to non-bridging bromide ions (N—H bonds essentially parallel to the layer). The third N—H...Br bond is to a bridging Br ion (the N—H bond in an

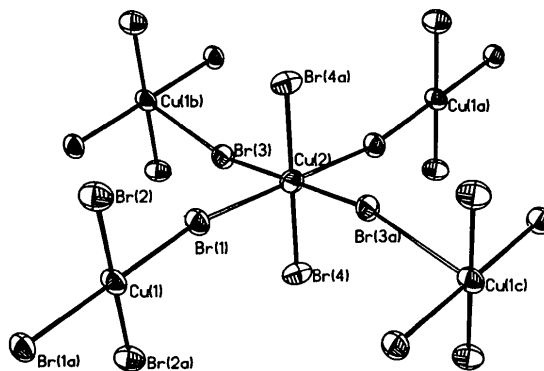


Fig. 1. Layer structure in $(C_3H_6N_2H_6)CuBr_4$. The a axis is horizontal.

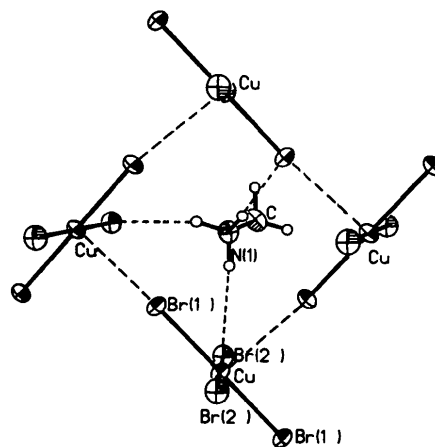


Fig. 2. Illustration of the relationship between the $-CH_2NH_3^+$ moieties and the halide layer in $(C_2H_4N_2H_6)CuBr_4$. View normal to c axis.

eclipsed conformation with the C atom). This is identical to the hydrogen-bonding scheme found in the neutron diffraction study of the corresponding chloride salt (Tichy *et al.*, 1978). The interlayer Br...Br distance is 3.602 Å, nearly 0.3 Å shorter than the sum of the van der Waals radii and 0.02 Å shorter than the Cl...Cl distance in the chloride salt. Thus this distance is dictated by the length of the cation rather than by halide-halide repulsions.

In contrast, the structures of the Cl and Br salts with the propylenediammonium cation are not isomorphous. The chloride salt (Phelps *et al.*, 1976) is orthorhombic with the propylenediammonium cation assuming an all-*trans* conformation and lying athwart a mirror plane passing through the central C atom. Thus the adjacent layers are precisely eclipsed. Because the propylenediammonium cation is fully extended, the Cl...Cl distance is quite long (4.548 Å). In the bromide structure, this mirror plane is lost, and the structure becomes monoclinic. Two independent centrosymmetric CuBr₄²⁻ anions are present in each layer and the semi-coordinate Cu...Br distances are substantially longer (3.148, 3.148 Å) than in the ethylenediammonium salt (3.034 Å). All of the atoms in the propylenediammonium cations lie in general positions and the cation backbone is no longer planar (Fig. 3), but the C(4)–N(5) bond assumes a *gauche* conformation with respect to the C(2)–C(3)–C(4) framework. Thus, the cation conformation is *tg* in contrast to the *tt* conformation in the chloride salt [the conformations in the *n* = 4 and *n* = 5 salts are *gtg* and *ttg* respectively (Garland *et al.*, 1989) for both *X* = Cl⁻ and *X* = Br⁻]. As seen in Fig. 4, one C–NH₃ end [the N(5) end] hydrogen bonds in a manner similar to that in the ethylenediammonium salt. However, the *gauche* bond existing at that end of the cation forces a different hydrogen-bond geometry at the other end with one N–H...Br bond to a terminal Br ion and two to bridging Br ions. This causes the layers to slide 1.03 Å out of the totally eclipsed configuration. More importantly, it moves the layers closer together and tilts the Cu(1) and Cu(2) chromophores in opposite senses (see

Fig. 3) so that the Br...Br interlayer contacts are only 4.063 Å. This latter distance is nearly 0.5 Å shorter than the corresponding Cl...Cl distance in (C₃H₆N₂H₆)CuCl₄. The increased intralayer repeat distance in the Br salt is presumably responsible for allowing the cation out of the all-*trans* conformation.

The presence of the *gauche* bond in the propylenediammonium ion has important consequences with respect to the crystallographic symmetry of the metal halide layers. Adjacent CuX₄²⁻ anions within the layer of the ethylenediammonium salts are related by an *a* glide perpendicular to the *b* axis. This structural feature is seen for almost all other previously reported antiferrodistortive (RNH₃)₂CuX₄ or (NH₃RNH₃)CuX₄ salts (upon appropriate transformation of the crystallographic axes) (Willett, Place & Middleton, 1988). The presence of two crystallographically independent NH₃⁺ groups in the propylene system destroys this symmetry element, leading to the presence of two independent CuBr₄²⁻ anions. The only other structures with this lowering of symmetry within the layer are in the [NH₃(CH₂)₂NH₃]CuX₄ (*X* = Cl, Br) system (Garland *et al.*, 1989).

One of the objects of the systematic study of the magnetic properties of materials is to delineate the origins of the magnetic behavior in terms of their structural and electronic properties (Willett, Gatteschi & Kahn, 1985). Copper(II) systems have been extensively studied in this respect because of their varied structural characteristics and the simplicity of their electronic structure. Table 5 tabulates the relevant structural and magnetic parameters for the first four members of the alkyldiammonium copper halide series and will provide data for several correlations.

The intralayer magnetic coupling, which occurs through a single halide ion and thus is denoted by *J*_{1*h*}, is ferromagnetic in nature since the magnetic orbitals on

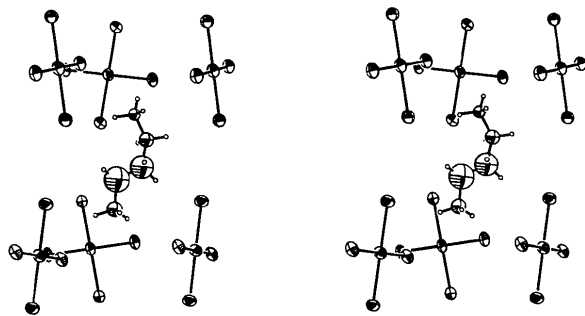


Fig. 3. Illustration of the conformation of the propylenediammonium ion. The *z* axis is to the left, *x* axis is down.

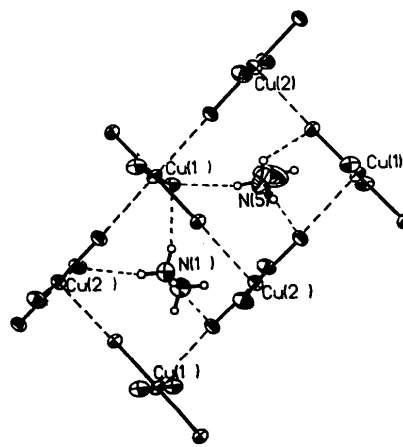


Fig. 4. Illustration of the relationship between the $-\text{CH}_2\text{NH}_3^+$ fragments and the halide layer in (C₃H₆N₂H₆)CuBr₄. View normal to *c* axis.

Table 5. *Structural and magnetic parameters for* $[\text{NH}_3(\text{CH}_2)_n\text{NH}_3]\text{CuX}_4$ *salts* ($n=2-5$)

$X = \text{Br}^-$									
n	Cu-Br (Å)	Cu...Br (Å)	Cu-Br...Cu (°)	J_{1h}/k (K)	Cu-Br (Å)	Br...Br (Å)	Cu-Br...Br (°)	J_{2h}/k (K)	References*
2	2.431	3.034	164.5	39	2.444	3.602	155.7	-68.4	RWHHD
3	2.444	3.148	164.0	26	2.440	4.063	155.8	-26	SHED
	2.431	3.148	165.6		2.450		174.2		
4	2.442	3.185	166.3	29	2.431	4.801	154.9	-5	GEP,SHED
5	2.429	3.164	164.2	23	2.442	6.234	167.3	-2	GEP,SHED
	2.430	3.179	166.3		2.450		149.2		
$X = \text{Cl}^-$									
n	Cu-Cl (Å)	Cu...Cl (Å)	Cu-Cl...Cu (°)	J_{1h}/k (K)	Cu-Cl (Å)	Cl...Cl (Å)	Cu-Cl...Cl (°)	J_{2h}/k (K)	References*
2	2.288	2.882	166.5	23.0	2.294	3.623	159.6	-13.7	TBHA,SSSED
3	2.275	2.946	165.7	15.4	2.314	4.548	171.3	-1.7	PLHH
4	2.308	3.100	166.2	13.0	2.280	4.941	154.8	-0.16	GEP,STD
5	2.279	3.058	164.5	14.1	2.299	6.525	167.6	-0.04	GEP,STD
	2.307	3.020	166.1		2.307		149.6		

* Letters are the initials of the last names of the authors.

adjacent CuX_4^{2-} anions are nearly orthogonal. This can be seen by the bridging $\text{Cu}-X\cdots\text{Cu}$ angles. For a given halide ion, the magnitude of J_{1h} depends on the extent of differential overlap between the two magnetic orbitals. Thus a strong dependence upon the semi-coordinate bond length is expected, as has been observed experimentally (Landee, Halvorson & Willett, 1987). The data in Table 5 readily confirm those ideas, with J_{1h} much larger for the ethylenediammonium salts, where the $\text{Cu}\cdots X$ distances are 0.1–0.2 Å shorter than in the other salts.

It is observed that $J_{1h}(\text{Br})$ is considerably larger than $J_{1h}(\text{Cl})$. It is possible that this is related to the increased delocalization of the unpaired electron out onto the halide ion in the CuBr_4^{2-} anion as compared to the CuCl_4^{2-} anion. This latter fact has been demonstrated by EPR studies of the Cu^{2+} ion doped into the K_2PdX_4 lattice ($X = \text{Cl}^-, \text{Br}^-$) (Chow, Chang & Willett, 1973; Aramuburu & Moreno, 1985). A similar ligand dependence has been observed for the antiferromagnetic contribution to the exchange coupling in bridged oligomers and chains (Willett, 1986; Scott & Willett, 1987) where this contribution is about twice as large for the Br complexes as for the Cl complexes. This latter effect has been ascribed to the lower energy of the charge-transfer transition in the Br salts.

The dependence of the interlayer magnetic coupling, which occurs *via* an exchange pathway involving two halide ions and thus is labeled J_{2h} , is strongly dependent upon the $X\cdots X$ contact distance between layers, the geometry of the $\text{Cu}-X\cdots X-\text{Cu}$ linkage, and upon the halide ion. In both the $X = \text{Cl}$ and the $X = \text{Br}$ series, $|J_{2h}|$ decreases monotonically with the $X\cdots X$ distance as can be seen in the $\ln-\ln$ plot in Fig. 5. However, the apparent slope of 6.5 for the Br salts is considerably smaller than the apparent slope of 10 for the Cl salts. In both series, the $n = 4$ point lies significantly below the best straight line. For the Cl series, the non-regular behavior has been attributed to changes in the non-

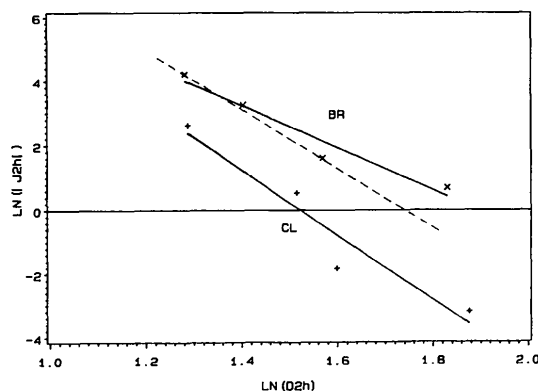


Fig. 5. Plot of $\ln |J_{2h}/k|$ vs $\ln d(X\cdots X)$ for $\text{NH}_3(\text{CH}_2)_n\text{NH}_3\text{CuX}$ salts. Solid lines: best least-squares lines for $X = \text{Br}$ (\times) and $X = \text{Cl}$ ($+$). Dashed line: line through $n = 2$ and $n = 4$ data points for $X = \text{Br}$.

linearity of the $\text{Cu}-X\cdots X$ interaction (Snively *et al.*, 1981; Block & Jansen, 1982; Straatman, Block & Jansen, 1984). Since the unpaired electron is primarily delocalized into ligand p_σ orbitals, the two-halide exchange interaction will be a maximum when the $\text{Cu}-X\cdots X$ angle is 180° . In fact, the calculation of Block & Jansen (1982) indicates this interaction drops off very rapidly as this angle deviates from 180° , with J_{2h} going to zero when the related $\text{Cu}\cdots\text{Cu}-X$ angle reaches 30° .

From examination of the non-regular variations in the $\text{Cu}-X\cdots X$ angles given in Table 5, a linear $\ln-\ln$ relation between $|J_{2h}/k|$ and d_{2h} (the $X\cdots X$ distance) cannot be expected. For the Br series, it is more appropriate to analyze the data in the following manner. The $n = 2$ and $n = 4$ Br salts have nearly equal $\text{Cu}-\text{Br}\cdots\text{Br}$ angles, and thus can be reasonably compared. A line through those data points gives a slope of 9 ± 0.6 (Straatman *et al.*, 1984). The $n = 3$ salt lies somewhat above this line, as would be predicted by the

larger average Cu—Br...Br angle. The data point for $n = 5$ lies further from the line than would be predicted from its geometrical parameters and it appears that the experimental value of $|J_{2h}|$ may have been overestimated for this latter case.

Straatman *et al.* (1984) have also shown that J_{2h} depends strongly upon the lengths of the Cu—X bonds involved in the two-halide bridges with $|J_{2h}|$ increasing as the Cu—X length shortens. For the bromide series, there is little variation in these lengths, so it would not appear to be an important factor. For the chlorides, in contrast, there are significant differences which need to be taken into account when discussing those correlations.

The authors acknowledge the support of NSF grant DMR-8219430. In addition, the X-ray diffraction facility was established through funds supplied by NSF grant CHE-8408407 and by The Boeing Company. Appreciation is expressed to Professor J. K. Garland for sharing results prior to publication.

References

- ARAMUBURU, J. A. & MORENO, M. (1985). *J. Chem. Phys.* **83**, 6071–6077.
- AREND, H., HUBER, W., MISCKOVSKY, F. H. & VAN LEEUWEN, G. R. K. (1978). *J. Cryst. Growth*, **43**, 213–223.
- BARENDREGT, F. & SCHENK, H. (1970). *Physica (Utrecht)*, **49**, 465–468.
- BLOCK, R. & JANSEN, L. (1982). *Phys. Rev. B*, **26**, 148–153.
- CAMPANA, C. F., SHEPHERD, D. F. & LITCHMAN, W. N. (1981). *Inorg. Chem.* **20**, 4039–4044.
- CHOW, C., CHANG, K. & WILLETT, R. D. (1973). *J. Chem. Phys.* **59**, 2629–2640.
- FERGUSON, G. L. & ZASLOW, B. (1971). *Acta Cryst.* **B27**, 849–852.
- GARLAND, J. K., EMERSON, K. & PRESSPRICH, M. (1989). Submitted.
- International Tables for X-ray Crystallography* (1974). Vol. IV. Birmingham: Kynoch Press. (Present distributor Kluwer Academic Publishers, Dordrecht, The Netherlands.)
- JONGH, L. J. DE & MIEDEMA, A. (1974). *Adv. Phys.* **23**, 1–260.
- LANDEE, C. P., HALVORSON, K. & WILLETT, R. D. (1987). *J. Appl. Phys.* **61**, 3295–3297.
- LARSEN, K. P. (1974). *Acta Chem. Scand. Ser. A*, **28**, 194–200.
- PHELPS, D. W., LOSEE, D. B., HATFIELD, W. E. & HODGSON, D. J. (1976). *Inorg. Chem.* **15**, 3147–3152.
- RUBENACKER, G. V., WAPLAK, S., HUTTON, S. L., HAINES, D. N. & DRUMHELLER, J. E. (1985). *J. Appl. Phys.* **57**, 3341–3342.
- SCOTT, B. & WILLETT, R. D. (1987). *J. Appl. Phys.* **61**, 3289–3291.
- SHELDRIK, G. M. (1985). *SHELXTL*. Version 5.1. Nicolet Instrument Corporation, Madison, WI, USA.
- SNIVELY, L. O., HAINES, D. N., EMERSON, K. & DRUMHELLER, J. E. (1982). *Phys. Rev. B*, **26**, 5245–5247.
- SNIVELY, L. O., SEIFERT, P. L., EMERSON, K. & DRUMHELLER, J. E. (1979). *Phys. Rev. B*, **20**, 2101–2104.
- SNIVELY, L. O., TUTHILL, G. & DRUMHELLER, J. E. (1981). *Phys. Rev. B*, **24**, 5349–5355.
- STEADMAN, J. P. & WILLETT, R. D. (1970). *Inorg. Chim. Acta*, **4**, 367–371.
- STRAATMAN, P., BLOCK, R. & JANSEN, L. (1984). *Phys. Rev. B*, **29**, 1415–1418.
- TICHY, K., BENES, J., HÄLG, W. & AREND, H. (1978). *Acta Cryst.* **B34**, 2970–2981.
- WILLETT, R. D. (1964). *J. Chem. Phys.* **41**, 2243–2244.
- WILLETT, R. D. (1986). *Inorg. Chem.* **25**, 1918–1920.
- WILLETT, R. D., GATTESCHI, D. & KAHN, O. (1985). Editors. *Magnetostructural Correlations in Exchange Coupled Systems*. Dordrecht: Reidel.
- WILLETT, R. D., PLACE, H. & MIDDLETON, M. (1988). *J. Am. Chem. Soc.* Accepted.

Acta Cryst. (1988). **C44**, 2076–2079

The Synthesis and Structure of (*N*-{2-[2-(2-Ammonioethylamino)ethylamino]ethyl}-salicylideneaminato-*O,N,N',N''*)nickel(II) Perchlorate

BY G. BRUNO, F. CUSMANO PRIOLO, F. NICOLÒ AND E. ROTONDO

Dipartimento di Chimica Inorganica e Struttura Molecolare, Università di Messina, Vill. S. Agata, salita Sperone 31, 98100 Messina, Italy

(Received 5 November 1987; accepted 13 May 1988)

Abstract. [Ni(C₁₃H₂₂N₄O)](ClO₄)₂, $M_r = 507.9$, triclinic, $P\bar{1}$, $a = 8.699$ (1), $b = 10.029$ (1), $c = 11.923$ (1) Å, $\alpha = 94.34$ (3), $\beta = 108.63$ (4), $\gamma = 96.10$ (3)°, $V = 973.4$ (4) Å³, $Z = 2$, $D_x = 1.73$ Mg m⁻³, $Mo K\alpha$, $\lambda = 0.71069$ Å, $\mu = 12.5$ cm⁻¹, $F(000) = 524$, $T = 298$ K, final $R = 0.055$ and $wR = 0.061$ for 2900 independent reflections [$I > 3\sigma(I)$]. The coordination polyhedron around Ni is an irregular square pyramid with the protonated saltrien [saltrien = 2-O⁻-C₆H₄CH=N(CH₂)₂NH(CH₂)₂NH(CH₂)₂NH₂]

acting as tetradentate ligand through one O and three N atoms.

Introduction. Structural, electronic and magnetic properties of Schiff-base coordination compounds have been measured in depth and form a significant part of our knowledge of the inorganic chemistry of chelate systems (Holm & O'Connor, 1971). In recent years Schiff-base complexes have been proposed as a model to describe energy transfer in naturally occurring systems,